ORGANIC LETTERS

2012
Vol. 14, No. 8
2094–2097

A New "Turn-on" Naphthalenedimide-Based Chemosensor for Mercury Ions with High Selectivity: Successful Utilization of the Mechanism of Twisted Intramolecular Charge Transfer, Near-IR Fluorescence, and Cell Images

Qianqian Li,[†] Ming Peng,[†] Huiyang Li,[†] Cheng Zhong,[†] Liang Zhang,[†] Xiaohong Cheng,[†] Xiaoniu Peng,[‡] Ququan Wang,[‡] Jingui Qin,[†] and Zhen Li*[,†]

Department of Chemistry and Department of Physics and Technology, Wuhan University, Wuhan 430072, China

lizhen@whu.edu.cn; lichemlab@163.com

Received March 12, 2012

ABSTRACT

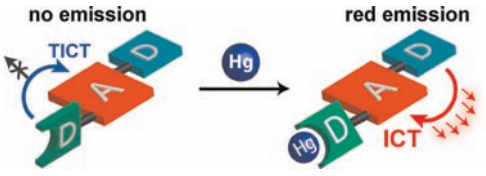

For the first time, a new near-IR "turn-on" fluorescent chemosensor with high selectivity for Hg^{2+} ions was designed according to the twisted intramolecular charge transfer (TICT) mechanism. The selective fluorescence enhancement effect can be optimized by modulating the solvent systems. And this naphthalenedimide-based sensor with long wavelength absorption and emission can be used to image intracellular Hg^{2+} ions in living Hela cells.

Nowadays, it is very important to detect some analytes, including ions, explosives, proteins, DNA, and RNA in certain samples for medical diagnosis, antiterrorism, environmental monitoring, etc. Thus, chemosensors, especially fluorescent ones with high sensitivity and low background disturbance, have attracted increased interest.[1] As required by biologists and medical experts, those with near-IR emission are welcome since the signal could easily penetrate the body tissue to facilitate detection and reduce damage.[2] Thanks to the enthusiastic efforts of scientists, many good chemosensors were reported, and some design rules have been summarized.[3] In addition to the frequently used fluorescence signaling mechanisms of photoinduced electron transfer (PET) and intramolecular charge transfer (ICT), the concept of twisted intramolecular charge transfer (TICT), proposed by Lippert and co-workers,[4] has seldom been utilized, possibly due to the difficulty of

[†] Department of Chemistry.
[‡] Department of Physics and Technology.

(1) (a) Gunnlaugsson, T.; Glynn, M.; Tocci, G. M.; Kruger, P. E.; Pfeffer, F. M. *Coord. Chem. Rev.* **2006**, *250*, 3094–3117. (b) Chen, X.; Zhou, Y.; Peng, X.; Yoon, J. *Chem. Soc. Rev.* 2010, *39*, 2120−2135, 3781 (c) Braunstein, P.; Naud, F. *Angew. Chem., Int. Ed.* **2001**, *40*, 680–699. (d) Dickinson, T. A.; White, J.; Kauer, J. S.; Walt, D. R. *Nature* **1996**, *382*, 697–700. (e) Maxwell, P. H.; Wiesener, M. S.; Chang, G. W.; Clifford, S. C.; Vaux, E. C.; Cockman, M. E.; Wykoff, C. C.; Pugh, C. W.; Maher, E. R.; Ratcliffe, P. J. *Nature* **1999**, *399*, 271–275. (f) Pichlmair, A; Schulz, O; Tan, C. P.; Naslund, T. I; Liljestrom, P.; Weber, F.; Sousa, C. R. E. *Science* **2006**, *314*, 997–1001.

(2) (a) Coskun, A.; Yilmaz, M. D.; Akkaya, E. U. *Org. Lett.* **2007**, *9*, 607–609. (b) Guo, Z.; Zhu, W.; Zhu, M.; Wu, X.; Tian, H. *Chem.—Eur. J.* **2010**, *16*, 14424–14432. (c) Hung, C. H.; Chang, G. F.; Kumar, A.; Lin, G. F.; Luo, L. Y.; Ching, W. M.; Diau, E. W. G. *Chem. Commun.* **2008**, *44*, 978–980. (d) Atilgan, S.; Ozdemir, T.; Akkaya, E. U. *Org. Lett.* **2008**, *10*, 4065–4067.

(3) (a) Coskun, A.; Akkaya, E. U. *J. Am. Chem. Soc.* **2006**, *128*, 14474–14475. (b) Cheng, T.; Xu, Y.; Zhang, S.; Zhu, W.; Qian, X.; Duan, L. *J. Am. Chem. Soc.* **2008**, *130*, 16160–16161. (c) Qian, F.; Zhang, C.; Zhang, Y.; He, W.; Gao, X.; Hu, P.; Guo, Z. *J. Am. Chem. Soc.* **2009**, *131*, 1460–1468.

(4) Lippert, E.; Lüder, W.; Moll, F.; Nagele, H.; Boos, H.; Prigge, H.; Siebold-Blankenstein, I. *Angew. Chem.* **1961**, *73*, 695–706.

10.1021/ol300607m
Published on Web 04/11/2012

controlling two crucial factors, the degree of the electron transfer and the change of molecular geometry. Correspondingly, the TICT-based fluorescent chemosensors are still very scarce (Chart S1, Supporting Information),[5] although in principle, the well-designed ones should show very good performance.

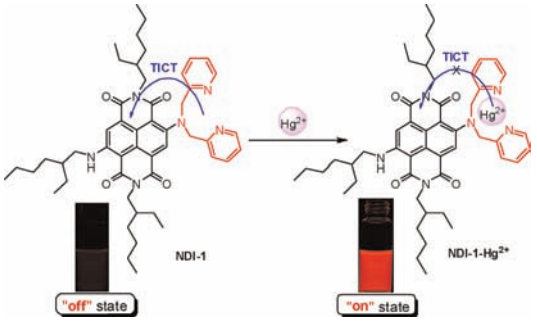

Figure 1. Hg^{2+}-ions suppress the TICT process of **NDI-1** for the detection of Hg^{2+} ions.

Mercuric ions (Hg^{2+}), one of the more severe environmental pollutants, are very harmful to humans. Specifically, methylmercury, yielded from the microbial biomethylation of Hg^{2+}, is known to cause brain damage and other chronic diseases. Hence, rapid and sensitive analysis of Hg^{2+} is badly needed.[6] Recently, according to the ICT mechanism, based on the protection reaction between ethanethiol and aldehyde, we have developed a new approach for the design of ratiometric fluorescent chemosensors for mercury ions (Chart S2, Supporting Information).[7] However, the emission ranges (450–550 nm) were rather far from the near-IR range. Based on our previous work, according to the TICT mechanism, we have elaborately designed a new "turn-on" naphthalenedimide (NDI)-based chemosensor (**NDI-1**, Figure 1) for Hg^{2+}, in which the core-substituted NDI acts as a fluorophore, di-2-picolylamine (DPA) acts as a receptor for Hg^{2+}, and an additional hexylamine unit was incorporated as a strong electron-donor to the NDI core to extend the push–pull electronic system of the whole molecule for the tuning of the emission to the desirable near-IR region. **NDI-1** nearly emitted nonluminescence in solution ("off" state) (Figure 1), as a result of the presence of the TICT state. Upon the addition of Hg^{2+}, the coordination between Hg^{2+} and the DPA group in **NDI-1** could restrain the formation of the TICT state, directly leading to strong red emission ("on" state) (Figure 1). To the best of our knowledge, this is the first time that a new near-IR fluorescent chemosensor with high selectivity for mercury ions was designed according to the TICT mechanism.

NDI-1 was easily prepared (Scheme S1, Supporting Information) and well characterized. The fluorescent measurements for **NDI-1** were first performed in THF solution. As shown in Figure S1 (Supporting Information), **NDI-1** had a visible absorption maximum wavelength at 592 nm and emitted very weakly (λ_{em} = 640 nm). This result was unexpected, since its analogue (Chart S3, Supporting Information) consisting of core-substituted NDI as the acceptor and butylamine unit as the donor exhibited strong fluorescence,[8] indicating that the DPA unit directly bound to the NDI core quenched the emission for the formation of the TICT state. Excitingly, upon the addition of Hg^{2+} ions, the fluorescent intensity of **NDI-1** increased rapidly, and 1.0 equiv of Hg^{2+} ions triggered a 110-fold enhancement. Correspondingly, its absorption maximum wavelength blue-shifted to 566 nm, with a clean isosbestic point of 574 nm. The apparent color change from blue to purple could be distinguished by the naked eye as shown in the inset of Figure S1 (Supporting Information). This fluorescent behavior was almost totally different from the recently reported NDI dyes (**PND**), which also contain DPA moieties as the acceptor (Chart S4, Supporting Information).[9] The differences of their structures were small; there was no spacer between the NDI core and the DPA group in **NDI-1**, while there was in **PND**. This seemingly ignorable difference directly led to the disparate properties because of the totally different internal mechanisms, PET for PND versus TICT of **NDI-1**. This phenomenon also partially confirmed that it was not easy to design new chemosensors according to the TICT mechanism, as mentioned above.

The interaction and binding behavior between **NDI-1** and Hg^{2+} ions were investigated with their ^1H NMR and ESI-MS spectra (Figures S2 and S3 and Table S1, Supporting Information). Similar to typical examples,[9] the signal of the hydrogen atoms in pyridine rings showed a significant downfield shift (up to $\Delta\delta$ = 0.66 ppm), indicating a charge transfer from the pyridine groups to the Hg^{2+} ions; meanwhile, the slightly downfield shifts of the hydrogen atoms in the NDI core, disclosing that the nitrogen atoms linked to the NDI core, have participated in the binding process with Hg^{2+} ions. Thus, all three nitrogen atoms in one DPA group interacted with the Hg^{2+} ions (Figure 1). To further clarify their relationship, calculations based on a time-dependent density functional theory (TDDFT) were conducted at the B3LYP/6-31G* level

(5) (a) Liu, Y.; Han, M.; Zhang, H.; Yang, L.; Jiang, W. *Org. Lett.* **2008**, *10*, 2873–2876. (b) Collins, G. E.; Choi, L. S.; Callahan, J. H. *J. Am. Chem. Soc.* **1998**, *120*, 1474–1478. (c) Aoki, S.; Kagata, D.; Shiro, M.; Takeda, K.; Kimura, E. *J. Am. Chem. Soc.* **2004**, *126*, 13377–13390. (d) Kollmannsberger, M.; Rurack, K.; Resh-Genger, U.; Daub, J. *J. Phys. Chem. A* **1998**, *102*, 10211–10220.

(6) (a) Kim, J. S.; Quang, D. T. *Chem. Rev.* **2007**, *107*, 3780–3799. (b) Valeur, B.; Leray, I. *Coord. Chem. Rev.* **2000**, *205*, 3–40. (c) Nolan, E. M.; Lippard, S. J. *Chem. Rev.* **2008**, *108*, 3343–3480. (d) Liu, L.; Zhang, G.; Xiang, J.; Zhang, D.; Zhu, D. *Org. Lett.* **2008**, *10*, 4581–4584. (e) Zhang, G.; Zhang, D.; Yin, S.; Yang, X.; Shuai, Z.; Zhu, D. *Chem. Commun.* **2005**, 2161–2163.

(7) (a) Cheng, X.; Li, S.; Jia, H.; Zhong, A.; Zhong, C.; Feng, J.; Qin, J.; Li, Z. *Chem.—Eur. J.* **2012**, *18*, 1691–1699. (b) Cheng, X.; Li, Q.; Li, C.; Qin, J.; Li, Z. *Chem.—Eur. J.* **2011**, *17*, 7276–7281. (c) Cheng, X.; Li, S.; Zhong, A.; Qin, J.; Li, Z. *Sensor. Actuat. B, Chem.* **2011**, *157*, 57–63. (d) Cheng, X.; Li, Q.; Qin, J.; Li, Z. *ACS Appl. Mater. Inter.* **2010**, *2*, 1066–1072.

(8) Würthner, F.; Ahmed, S.; Thalacker, C.; Debaerdemaeker, T. *Chem.—Eur. J.* **2002**, *8*, 4742–4750.

(9) Lu, X.; Zhu, W.; Xie, Y.; Li, X.; Gao, Y.; Li, F.; Tian, H. *Chem.—Eur. J.* **2010**, *16*, 8355–8364.

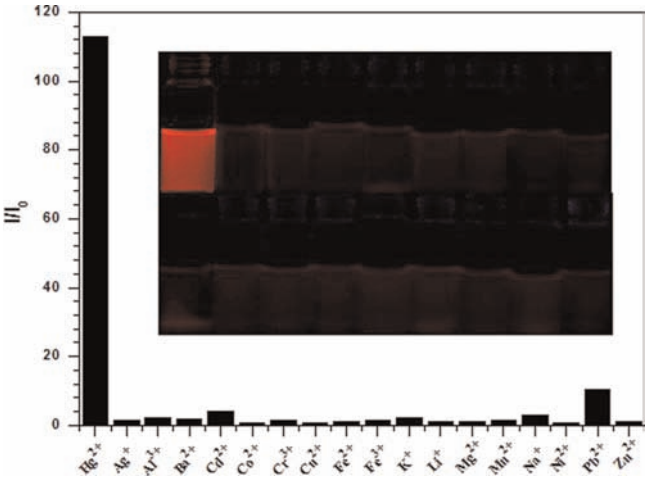

Figure 2. Fluorescence spectra profiles of **NDI-1** in THF (λ_{em} = 610 nm, 20 μM) with various metal ions (20 μM). Inset: fluorescence photograph of compound **NDI-1** with various metal ions (1.0 equiv), from left to right, Hg^{2+}, Ag^{+}, Al^{3+}, Ba^{2+}, Cd^{2+}, Co^{2+}, Cr^{3+}, Cu^{2+}, Fe^{2+}, Fe^{3+}, K^{+}, Li^{+}, Mg^{2+}, Mn^{2+}, Na^{+}, Ni^{2+}, Pb^{2+}, Zn^{2+}.

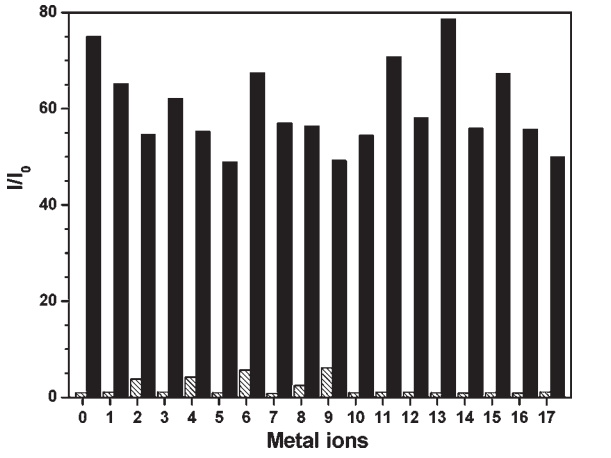

Figure 3. Fluorescence spectra profiles of **NDI-1** in acetone–water (1:1, v/v, 20 μM) with various metal ions. Strip bars represent the addition of the analytes (20 μM): (0) Free compound **NDI-1**, (1) Ag^{+}, (2) Al^{3+}, (3) Ba^{2+}, (4) Cd^{2+}, (5) Co^{2+}, (6) Cr^{3+}, (7) Cu^{2+}, (8) Fe^{2+}, (9) Fe^{3+}, (10) K^{+}, (11) Li^{+}, (12) Mg^{2+}, (13) Mn^{2+}, (14) Na^{+}, (15) Ni^{2+}, (16) Pb^{2+}, (17) Zn^{2+}. Black gray bars represent the subsequent addition of Hg^{2+} (20 μM) to the solution.

with the Gaussian 09 program[10] to explain the electronic structural properties of the ground and excited states behavior of **NDI-1** and NDI-1-Hg^{2+}. As shown in Figure S4 (Supporting Information), in the ground state, the optimized structure of **NDI-1** has a little dihedral angle about 35° between the NDI core and the DPA unit, and the hexylamine unit was nearly coplanar to the NDI core. The HOMO was delocalized through the whole π system, while the LUMO located in the NDI core resulted in the "D(donor)–A(acceptor)–D" system. However, in the first excited state, for the large degree of electron transfer between the donor (the DPA unit) and acceptor (the NDI core), the TICT state, also the nonradiative excited state, was formed. In this case, the DPA unit was nearly perpendicular to the NDI core, and the HOMO was restricted on the DPA unit, while the LUMO was located in the NDI core, leading to the charge separation state between the donor and acceptor. Thus, the TICT states of the rotors caused nearly no fluorescence emission of **NDI-1**.

Upon the addition of Hg^{2+}, the binding of Hg^{2+} with the DPA unit decreased its electron donor ability, as proven by the blue-shifted absorption peak. Also, the formation of the **NDI-1**–Hg^{2+} complex induced the enlargement of the dihedral angle between the NDI core and the DPA unit, further decreasing their electron transfer. As shown in Figure S5 (Supporting Information), in the complex of **NDI-1** and Hg^{2+} ions, both of the LUMO and HOMO almost focused on the NDI and hexylamine moieties and the optimized structure nearly remained the same either in the ground state or the first excited state. Thus, the binding of Hg^{2+} prohibited the TICT formation of **NDI-1**, largely promoting the strong red fluorescence emission, as observed in Figure S1 (Supporting Information).

To further understand the TICT mechanism and study the effect of the molecular motion on charge transfer at an excited state, the fluorescence intensity dependence on solvent and the effect of the solvent viscosity and temperature were assessed (Figures S6–S8, Supporting Information). The obtained experimental results confirmed that the excited state of **NDI-1** was decayed by the TICT process and the cooperative binding of Hg^{2+} through a DPA moiety could restrain the formation of the TICT state efficiently, leading to the "turn-on" fluorescence response of **NDI-1**.

To evaluate the specificity of **NDI-1** toward Hg^{2+}, various ions were examined in parallel under the same conditions. As shown in Figure 2, the binding of **NDI-1** with Hg^{2+} ions resulted in a 110-fold increase of the fluorescence intensity, whereas Ag^{+}, Al^{3+}, Ba^{2+}, Cd^{2+}, Co^{2+}, Cr^{3+}, Cu^{2+}, Fe^{2+}, Fe^{3+}, K^{+}, Li^{+}, Mg^{2+}, Mn^{2+}, Na^{+}, Ni^{2+}, Pb^{2+}, and Zn^{2+} had negligible influence. However, when 1.0 equiv of Hg^{2+} was added into the THF solution of **NDI-1** in the presence of one of the other metal ions (1.0 equiv), the selectivity was interfered with by

(10) Gaussian 09, Revision E.1: Frisch, M. J.; Trucks, G. W.; Schlegel, H. B.; Scuseria, G. E.; Robb, M. A.; Cheeseman, J. R.; Montgomery, J. A., Jr.; Vreven, T.; Kudin, K. N.; Burant, J. C.; Millam, J. M.; Iyengar, S. S.; Tomasi, J.; Barone, V.; Mennucci, B.; Cossi, M.; Scalmani, G.; Rega, N.; Petersson, G. A.; Nakatsuji, H.; Hada, M.; Ehara, M.; Toyota, K.; Fukuda, R.; Hasegawa, J.; Ishida, M.; Nakajima, T.; Honda, Y.; Kitao, O.; Nakai, H.; Klene, M.; Li, X.; Knox, J. E.; Hratchian, H. P.; Cross, J. B.; Adamo, C.; Jaramillo, J.; Gomperts, R.; Stratmann, R. E.; Yazyev, O.; Austin, A. J.; Cammi, R.; Pomelli, C.; Ochterski, J. W.; Ayala, P. Y.; Morokuma, K.; Voth, G. A.; Salvador, P.; Dannenberg, J. J.; Zakrzewski, V. G.; Dapprich, S.; Daniels, A. D.; Strain, M. C.; Farkas, O.; Malick, D. K.; Rabuck, A. D.; Raghavachari, K.; Foresman, J. B.; Ortiz, J. V.; Cui, Q.; Baboul, A. G.; Clifford, S.; Cioslowski, J.; Stefanov, B. B.; Liu, G.; Liashenko, A.; Piskorz, P.; Komaromi, I.; Martin, R. L.; Fox, D. J.; Keith, T.; M. A. Al-Laham, Peng, C. Y.; Nanayakkara, A.; Challacombe, M.; Gill, P. M. W.; Johnson, B.; Chen, W.; Wong, M. W.; Gonzalez, C.; Pople, J. A. Gaussian, Inc., Pittsburgh, PA, 2009.

Co^{2+}, Cu^{2+}, and Ni^{2+} (Figure S9, Supporting Information). As mentioned above, in the TICT process, the positive and negative charges were located in two different and separated functional parts of **NDI-1**, with an increase in the molecular dipole moment, and the high polarity solvent could induce this process and stabilize the charge separated state.[5b] Thus, in principle, different solvents with different polarities should affect the emission spectra of **NDI-1**, especially the intensity, to some degree (Figure S6, Supporting Information). In other words, the change of the solvent might be a method to improve the selectivity for Hg^{2+}. After the relatively systematic tests in various solvents, we chose a mixture of acetone and water as the solvent system for **NDI-1** to detect Hg^{2+}, with the best ratio of 1:1 (v/v). As shown in Figure S10 (Supporting Information), only a small change appeared upon the addition of other metal ions, but a strong fluorescence response was observed with the subsequent addition of Hg^{2+}, exhibiting good selectivity for Hg^{2+} ions in the complicated systems.

The fluorescence emission of **NDI-1** over a wide range of pH values was studied (Figure S11, Supporting Information). No apparent changes of the fluorescence spectra were observed when the pH values ranged from 4.0 to 13.0, and the detection of Hg^{2+} can work well in in the range of pH 5.0−9.0 (Figure S11, Supporting Information). The selectivity of **NDI-1** to Hg^{2+} was also examined in the presence of various metal ions in these pH values. As shown in Figure S12 (Supporting Information), **NDI-1** still worked well and exhibited good selectivity. It should be pointed out that the stable fluorescence and good selectivity of **NDI-1** at a pH value of ~7.0 was favorable for the in vivo application. Thus, once more, the fluorescence titrations of **NDI-1** with Hg^{2+} were conducted under the optimized conditions (acetone/water = 1/1 (v/v), pH = 7.0), with the results summarized in Figure S13 (Supporting Information). Accompanying the increase of the concentration of the added Hg^{2+} ions, an obvious "turn-on" process of the fluorescence intensity at 610 nm was observed, and the maximum intensity was achieved: a 100-fold enhancement. As shown in Figure 3, the emission profile of the **NDI-1**−Hg^{2+} complex was unperturbed in the presence of 1.0 equiv of other metal ions. Additionally, the counteranions did not have obvious influences on the fluorescence spectra (Figure S14, Supporting Information).

The good performance of **NDI-1** prompted us to utilize it in the image of the HL cells by a confocal laser scanning microscopy. Bright-field measurements confirmed that the cells after treatment with Hg^{2+} and **NDI-1** were viable throughout the imaging experiments (Figure 4D−F). Under selective excitation of **NDI-1**, staining HL cells with a 2.5 μM solution of **NDI-1** for 10 min led to very weak intracellular fluorescence (Figure 4B), followed by the addition of Hg^{2+} (2.5 μM) for another 10 min; the apparent enhancement of fluorescence was easily observed (Figure 4C), suggesting that **NDI-1** can penetrate the cell membrane and be used for imaging of Hg^{2+}.

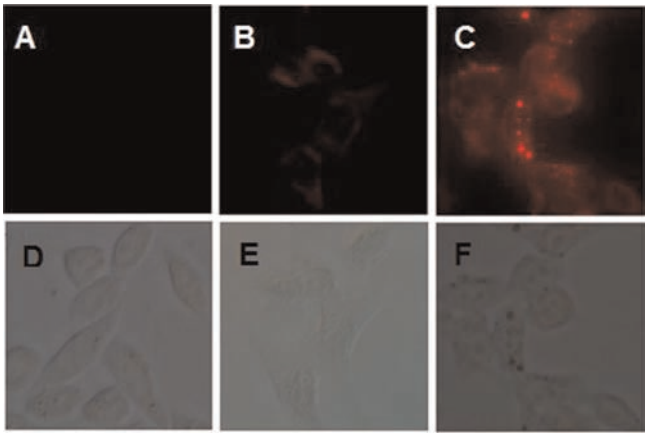

Figure 4. Confocal fluorescence images of living HL cells: (A) HL cells incubated with Hg^{2+} (5 μM) for 10 min; (B) HL cells cells incubated with compound **NDI-1** (2.5 μM) for 10 min; (C) HL cells incubated with **NDI-1** (2.5 μM) for 10 min after preincubation with Hg^{2+} (2.5 μM) for 10 min. (D), (E), and F) represent the bright-field images of (A), (B), and (C), respectively.

In conclusion, **NDI-1** has been designed according to the TICT mechanism, which exhibited "turn-on" fluorescence response toward Hg^{2+} ions. Coupled with the long wavelength fluorescence, cell-permeability, and its function in the wide range of pH, **NDI-1** can be applied to image Hg^{2+} ions in living cells and in vivo potentiality. And actually, for the even better performance, the structure of **NDI-1** should be further modified to improve the solubility in aqueous solutions. Thus, this good example might stimulate wide interest of scientists for further development of new chemosensors possessing excellent performance with the guidance of the TICT mechanism.

Acknowledgment. We are grateful to the National Science Foundation of China (No. 21002075) and the National Fundamental Key Research Program (2011CB932702) for financial support.

Supporting Information Available. Experimental section, fluorescence spectra, MS spectra, and ^{1}H NMR and ^{13}C NMR spectra. This material is available free of charge via the Internet at http://pubs.acs.org.

The authors declare no competing financial interest.